Removal of Moisture Contamination from Porous Polymeric Low-k Dielectric Films

Asad Iqbal, Harpreet Juneja, Junpin Yao, and Farhang Shadman
Dept. of Chemical Engineering, University of Arizona, Tucson, AZ 85721

DOI 10.1002/aic.10760
Published online January 4, 2006 in Wiley InterScience (www.interscience.wiley.com).

Ultra low-k dielectrics are expected to replace SiO_2 as the interlayer dielectric for the next-generation microelectronic devices. A challenge facing the integration of these dielectrics in manufacturing is their interactions with gaseous contaminants, such as moisture, and the resulting change in their properties. The physical and chemical interactions of moisture with porous spin-on dielectric material are investigated using temperature- and concentration-programmed exposure and purge sequence together with trace moisture analysis, using atmospheric pressure ionization mass spectrometry. The model compound in this study is methylsilsesquioxane, deposited and treated under typical manufacturing conditions. A process model is developed that provides information on the mechanism and kinetics of moisture uptake and release in thin porous films. The model elucidates the effect of film properties on the contamination uptake as well as outgassing; it also provides a valuable tool for designing an optimum process for contamination control and removal in porous films. © 2006 American Institute of Chemical Engineers *AIChE J,* 52: 1586–1593, 2006

Keywords: dielectrics, moisture, outgassing, methylsilsesquioxane (MSQ), desorption

Introduction

The continuing decrease in the dimensions of microelectronics devices presents significant manufacturing complexities and challenges.[1] So far, silicon dioxide has been the dielectric of choice as interlayer dielectric material. However, with the decrease in feature size, SiO_2 is rapidly approaching its limits in satisfying the required dielectric properties. For Moore's Law (doubling of the number of transistors every 18 months) to continue, new interlayer low dielectric constant (low-k) materials are needed to address problems in power consumption, signal propagation delays, and cross talk between interconnects in the next generation of integrated circuits.[2]

Resistance–capacitance (RC) delay could be reduced by the integration of Cu with low-k dielectrics.[3-5] Substitution of SiO_2 with low-k materials can reduce the RC delay by up to 75% for materials with k values close to 1.[6] Wide varieties of low-k dielectric materials, which are now available, can be both porous and nonporous. They can be classified into two main groups: Si-containing (or more precisely, Si–O-containing) and non–Si-containing (mostly organic polymers). The former can be further divided into two subgroups: silica-based and silsesquioxane-based.[7,8] Implementation of low-k dielectrics in a manufacturing environment requires an understanding of these new materials' characteristics and the challenges that appear in the integration of the low-k film into semiconductor processes. Besides their poor mechanical and thermal stability,[9-11] another disadvantage is their ability to absorb chemicals, such as contaminants containing polar O–H bonds arising from their porous structure. Even a small amount of absorbed moisture can increase the total k value, given that the k value of water is as high as 79.[7]

The properties of interlayer dielectric films are sensitive to the presence of homogeneous contaminants from various sources, which can in turn affect the process yield and degrade the final device performance. Moisture and organics are among the most detrimental because of their high reactivity with material surfaces. To design a process that minimizes the

Correspondence concerning this article should be addressed to F. Shadman at shadman@erc.arizona.edu.

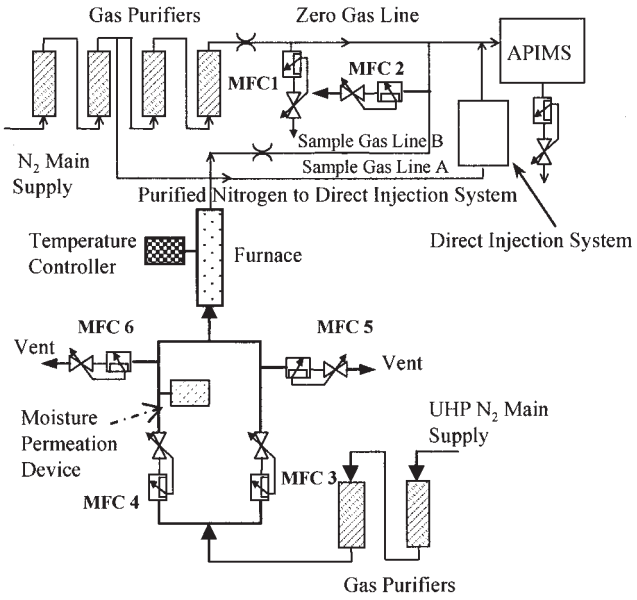

Figure 1. Experimental setup.

impact of moisture and organic contamination, it is necessary to have a fundamental understanding of the interactions between gaseous contaminants and the dielectric surface. Therefore, understanding the transport of gases through these low-k dielectric materials will help in designing better processes for integration of low-k material in semiconductor processing.

There has been a considerable amount of research on the interactions of contaminants with high-k dielectrics[12-14]; however, the mechanism of contaminant adsorption and diffusion in low-k materials and the effect of porosity and pore structure on the mobility of contaminants have not been adequately studied and characterized. This information is critical because these materials are exposed to a wide variety of conditions during fabrication processes. It is well known that moisture incorporated into a dielectrics matrix interacts chemically with the dielectric and exists in a variety of forms including both dissolved and reacted forms.[15,16] However, the dissociated and reacted water undergoes reverse reaction when moisture is desorbed and removed from the matrix. Although the nature of intermediate compounds formed in the matrix is important, the key parameters of interest for manufacturing are the overall uptake of moisture. Therefore, it is common to use the term "incorporated" (or "sorbed") moisture to refer to all by-products of moisture interactions with the matrix.

In this article a process model is set up to describe the mass transport of moisture in the polymer matrix and the pores (voids). A series of physical and geometric parameters have been estimated, and the effect of porosity and film thickness are discussed. The results predicted by the model agree well with the experimental data.

Experimental

Setup

Figure 1 shows the experimental setup used to study the interactions of trace levels of moisture with porous low-k dielectric films. An atmospheric pressure ionization mass spectrometer (APIMS) system was set up and used to monitor the gas-phase concentration of moisture. This system has the ability to detect impurities at ambient pressure with high sensitivity [in single-digit parts per trillion (ppt) range] and fast response time, thus allowing the study of adsorption/desorption kinetics at atmospheric pressure under flow conditions.

The gas mixing zone was designed to allow delivery of purge gas as well as challenge mixture (carrier, N_2 gas plus controlled level of moisture) in a well-defined, rapid, and controlled manner to the test reactor. Accurate calibrated gas mixtures could also be prepared using the gas-mixing setup. Errors resulting from dead volumes were minimized by eliminating stagnant parts and by continuously maintaining gas flow through the entire system. The gas delivery lines, made of electropolished stainless steel (EPSS), were heated to minimize moisture memory effects. The packed-bed reactor containing the wafer coupons was kept at a controlled temperature using a programmable furnace.

The test samples for this study were methylsilsesquioxane (MSQ) low-k dielectrics (JSR 5109, JSR Corp., Austin, TX) with a dielectric constant of 2.2–2.3. Wafers (8 in.) underwent the following processes: 0.55 μm thermal oxide (wet oxidation), 0.35 μm LPCVD nitride (thermal nitride on both sides of wafers), 0.40 μm Blanket JSR 5109, standard JSR cure, partial etch, and finally partial ash. The dielectric film had a porosity of 48% with an average pore diameter of 3 nm. The wafers were diced to produce 1 $\times$ 2-cm coupons, which were then loaded onto nickel-coated stainless steel springs and then randomly packed in a tubular Pyrex® reactor. This arrangement provided complete mixing of gases, and thus the reactor could be treated as a differential reactor. The total sample surface area was 648 cm^2.

Procedure

The experimental procedure consisted of the following steps: initial purge and bake, isothermal sorption (that is, incorporation of moisture) and desorption of moisture from samples, followed by a purge and a sequence of bake. Before each experiment, the reactor was purged and baked under ultrapure nitrogen up to 300°C to desorb any residual contaminants from the wafer surface. The sorption cycle involved exposure of the sample to a constant temperature and challenge moisture concentration until equilibrium was attained. The desorption cycle was initiated by switching to ultrapure nitrogen purge. Isothermal desorption was carried out at the same temperature as the sorption cycle. When the moisture concentration in the reactor outlet gas reached the background level, the reactor was heated to a higher temperature to speed up desorption rate. This stepwise purge and bake was carried out successively up to 300°C. Sorption experiments were carried out at different temperatures from 30 to 250°C and for concentrations from 56 to 165 ppb (parts per billion).

Results and Discussion

Figure 2 shows typical experimental results for interaction of moisture with porous MSQ or p-MSQ dielectric film (MSQ matrix and pores). The results give a temporal profile of the reactor outlet concentration during the sorption/desorption cycle. The total amount of moisture incorporated in the film is

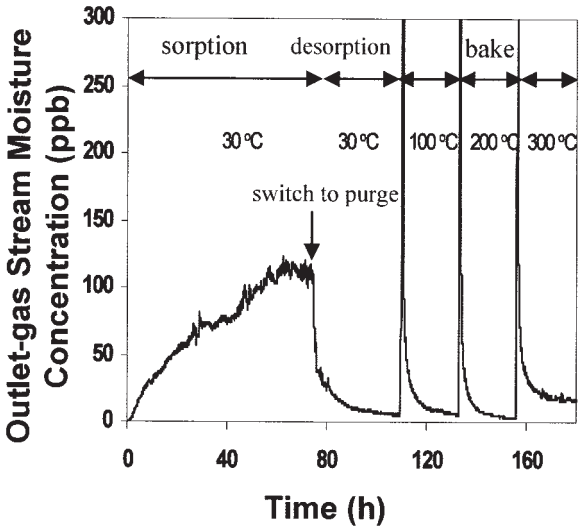

Figure 2. Temporal profile of sorption (challenge 111 ppb moisture), followed by temperature-programmed desorption.

calculated using the area above the sorption curve. Similarly, the area under the desorption curve gives the amount of moisture desorbed during the isothermal purge. The results show that extensive bake out is needed to remove most of the moisture left in the film after an isothermal desorption process.

Figure 3 shows the normalized reactor outlet concentration when samples are exposed to 165 ppb moisture challenge concentration at three different temperatures. Slight variations in the mass spectrometer readouts are attributed to sensitivity to variations in the gas flow rate and the ambient temperature. However, these variations are secondary and transient effects and do not affect the overall profile, average values over a long time, and trends. Figure 3 also indicates a delay in response, which is significant at 30°C but less pronounced at higher temperatures. This delay is much greater than the residence time of the reactor and therefore is not a result of reactor

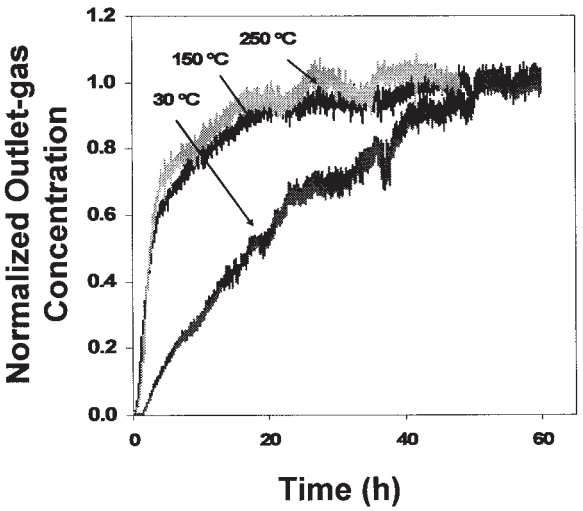

Figure 3. Temporal profiles of sorption (challenge 165 ppb moisture) at different temperatures.

Table 1. Experimentally Determined Solubility Values at Three Different Temperatures

Temperature (°C)	Solubility
30	2.75e7
150	9.66e6
250	6.99e6

breakthrough. The delay is caused by rapid and complete removal of moisture from the challenge gas early in the process while the p-MSQ surface is totally dry and fast sorbing. At higher temperatures, the desorption rate becomes more favorable; thus this initial rapid sorption and therefore the related delay in response become less noticeable.

Another observation made is that, under the same exposure time and challenge moisture concentration, the total amount of moisture sorbed is higher at lower temperatures. At lower temperatures, the sorption rate is higher than the desorption rate; this results in a more favorable equilibrium toward sorption and retention of moisture in the film. The difference in the net sorption profiles at different temperatures, as depicted in Figure 3, can also be explained by the same effect. However, there is another way that temperature affects the observed sorption and retention, based on the solubility of moisture in the MSQ matrix. Table 1 gives the solubility values at three different temperatures and indicates that solubility decreases with increase in temperature. The solubility factor S is given as a ratio of equilibrium matrix moisture concentration C_{s0} and gas-phase moisture concentration C_{gb0}. Moisture in the matrix is present in a wide variety of physical and chemical forms. As stated earlier, the term "moisture" in MSQ refers to the moisture equivalent of all intermediate compounds formed as a result of physical and chemical interactions with MSQ.

Capacity of the MSQ matrix for moisture retention decreases with temperature, which results in earlier breakthrough and steeper initial profiles as observed in Figure 3. For example, results show that changing temperature from 150 to 250°C only slightly changes the sorption profile compared to the change observed by increasing from 30 to 150°C. This is explained by the fact that dependency of solubility on temperature decreases with increasing temperature.

Based on the sorption profile, the film loading (total number of molecules per unit volume of the film) has been calculated. Because the wafer used in the experiment was coated with p-MSQ on one side and nitride on the other, the loading from the nitride surface assumed to behave similar to silicon dioxide have been separately evaluated and subtracted.[12] Figure 4 compares the moisture loading on p-MSQ film for a given challenge concentration and temperature with that of silicon dioxide. To compare the loadings, p-MSQ film loading was converted to molecules per unit area of the film. The results show that the amount of moisture sorbed in p-MSQ film is much greater than SiO_2 surface, primarily because of the structure and porosity of the p-MSQ film. At equilibrium the solubility at a given temperature and concentration is calculated using the following equation:

$$C_{\text{film0}} = C_{gp0}\varepsilon + C_{s0}(1-\varepsilon) \tag{1}$$

where C_{film0} is the loading in moisture molecules per unit volume of the film and C_{gp0}, the moisture concentration in the

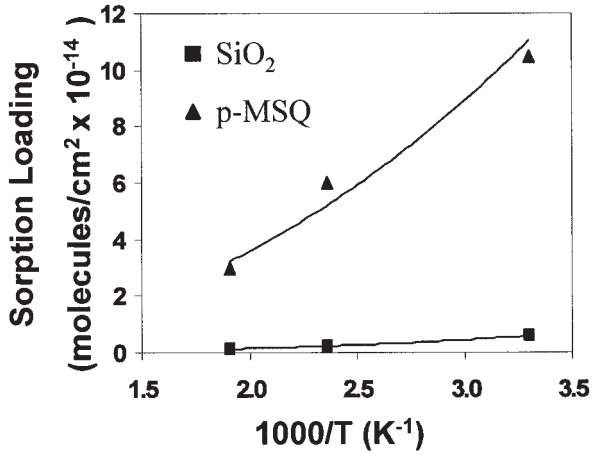

Figure 4. Comparison of moisture uptake in SiO_2 and p-MSQ, exposed to 56 ppb moisture.

pore, is equal to the challenge concentration C_{gb0}. C_{s0} is given by $C_{gb0}S$ because the matrix moisture concentration is in equilibrium with the gas-phase concentration, ε is the film porosity, and S is the solubility of moisture in the film.

Mathematical Modeling

Extensive literature is available on diffusion and permeation of gases in polymers and porous media.[17-21] Several authors have also studied reaction and diffusion of gases in silica.[22-26] However, the transport of moisture in porous dielectric polymers, such as porous MSQ, has unique features not represented by the available models. The proposed model represents the removal of moisture from p-MSQ film during the isothermal desorption process. As shown in Figure 5, the process of transport in porous low-k film is assumed to consist of the following simultaneous steps:

(1) Local exchange of moisture between the gas phase (including the gas in the pores) and the solid matrix across the gas–solid interphase. This exchange in general consists of both physisorption and dissociative chemisorption (such as hydroxylation), leading to formation of what is called "sorbed" moisture; the reverse process will be recombination and desorption back to the gas-phase moisture.

(2) Transport of sorbed moisture in the solid matrix by activated diffusion.

(3) Transport of molecular moisture in micropores by diffusion.

The governing equation for transport of moisture in the matrix is

$$D_s \frac{\partial^2 C_s}{\partial z^2} - \frac{S_p \varepsilon}{(1-\varepsilon)} k_m (C_s - C_{gp}S) = \frac{\partial C_s}{\partial t} \qquad (2)$$

The initial and boundary conditions for Eq. 2 are as follows:

Initial Condition

$$C_s = C_{gb0}S \qquad \text{at } t = 0 \qquad (2a)$$

Boundary Condition 1

$$\frac{\partial C_s}{\partial z} = 0 \qquad \text{at } z = 0 \qquad (2b)$$

Boundary Condition 2

$$-D_s \frac{\partial C_s}{\partial z} = k_{ms}(C_s - C_{gb}S) \qquad \text{at } z = L \qquad (2c)$$

where C_s is the aggregate concentration (moisture equivalent) of all intermediate species formed from reaction and incorporation of moisture with the low-k matrix; D_s is the effective diffusivity of moisture in the matrix and is defined and calculated based on flux of the overall moisture equivalent of these intermediate species; C_{gb} is concentration of moisture in the gas phase; k_m is the interphase transfer coefficient between the matrix and voids; k_{ms} is the interface transfer coefficient between the matrix and the gas phase in the surrounding medium (bulk gas); S_p is the specific surface area of the porous film; and L is thickness of the film. It is assumed that at equilibrium the concentration of moisture in the matrix is proportional to the moisture concentration in the gas phase (Henry's law equivalent).

The governing equation for the transport of moisture in pores is given by

$$D_g \frac{\partial^2 C_{gp}}{\partial z^2} + S_p k_m (C_s - C_{gp}S) = \frac{\partial C_{gp}}{\partial t} \qquad (3)$$

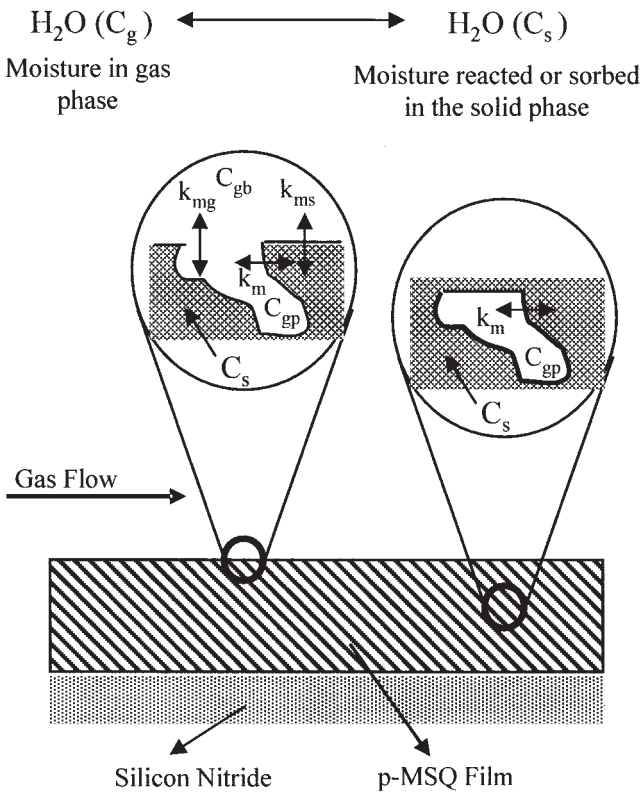

Figure 5. Moisture transport pathways in porous low-k films.

The initial and boundary conditions for Eq. 3 are as follows:

Initial Condition

$$C_{gp} = C_{gb0} \qquad \text{at } t = 0 \tag{3a}$$

Boundary Condition 1

$$\frac{\partial C_{gp}}{\partial z} = 0 \qquad \text{at } z = 0 \tag{3b}$$

Boundary Condition 2

$$-D_g \frac{\partial C_{gp}}{\partial z} = k_{mg}(C_{gp} - C_{gb}) \qquad \text{at } z = L \tag{3c}$$

where C_{gp} is the concentration of moisture in the pores, D_g is the gas-phase diffusivity of moisture in pores, and k_{mg} is the interphase transfer coefficient between pores and gas phase in the surrounding medium.

In the present study, the sorption and desorption of moisture with wafers took place in a packed bed of wafer modules arranged and oriented randomly. This reactor was assumed to behave as a differential reactor. This achieved a high degree of mixing, justifying a well-mixed reactor model and the following overall mass balance equation:

$$V\frac{dC_{gb}}{dt} = Q(C_{gb,in} - C_{gb}) + (1-\varepsilon)A_{tot}k_{ms}(C_s - C_{gb}S)\big|_{z=L} + \varepsilon A_{tot}k_{mg}(C_{gp} - C_{gb})\big|_{z=L} \tag{4}$$

where the first term represents change in the moisture concentration with time, the second term is the change in concentration of moisture arising from incoming and outgoing gas flow, the third term accounts for the moisture desorbed from matrix to gas phase at boundary $z = L$, and the fourth term represents the moisture desorbed from pore to gas phase at $z = L$. Q is the volumetric flow rate, V is volume of reactor, $C_{gb,in}$ is the concentration of moisture in inlet purge gas stream that is <1 ppb during isothermal desorption process, and A_{tot} is total exposed surface area available for moisture sorption.

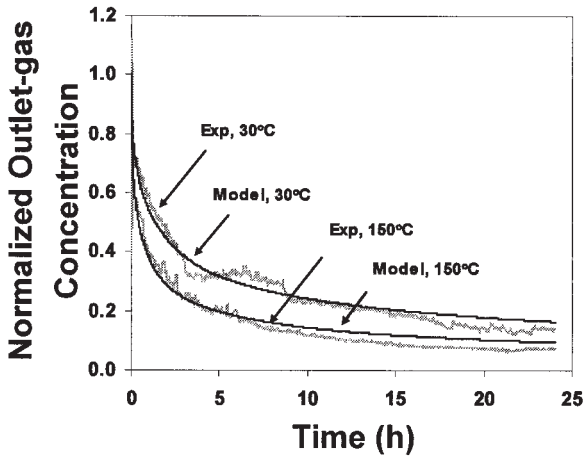

Figure 6. Comparison of model predictions and experimental data on outgassing profiles.

Sample exposed to and equilibrated with 56 ppb moisture before desorption.

Table 2. Parameters Estimated by Fitting Model to Experimental Desorption Data for 56 ppb Moisture Challenge

	Temperature (°C)		
Variable	30	150	250
D_s, cm^2/s	1.4e-15	1.7e-15	3.5e-15
D_g, cm^2/s	8.5e-10	1.0e-9	3.0e-9
k_m, cm/s	5.0e-13	5.0e-13	5.0e-13
k_{ms}, cm/s	1.0e-8	1.0e-8	1.0e-8
k_{mg}, cm/s	1.0e-7	1.0e-7	1.0e-7
S	3.65e7	1.9e7	1.0e7

Differential Eqs. 2–4 were solved numerically using a finite-element method. The model parameters D_s, D_g, k_m, k_{ms}, k_{mg}, and S were determined by fitting the model to the experimental data. In addition to describing the process qualitatively and providing a tool for extracting the fundamental parameters from the experimental data, the model can be used to predict the amount of moisture retained in such thin films when exposed to moisture in various environments. In practice, it is important to remove contaminants, including moisture, from these films; the model can also be used in these cases to design an optimum cleaning process either by isothermal or by temperature-programmed desorption, outgassing, and drying. The next section describes modeling results and predicts data for which experiments were not performed.

Modeling Results and Predictions

Application of the proposed model indicates that outgassing of moisture from porous MSQ film follows three distinct pathways:

(1) Exchange of moisture molecules between MSQ matrix and the pores

(2) Desorption of moisture from MSQ matrix to the bulk gas

(3) Diffusion of moisture out of the pores

The model described in the previous section was used to analyze the raw data and extract the fundamental process parameters. Figure 6 shows the model fit to data for only one set of conditions at two temperatures, 30 and 150°C. Agreement between the model and the experimental data is good. Similar results were obtained for other temperatures and challenge concentrations. The results of analysis and parameter estimation are summarized in Table 2. The transport through pores is not purely Knudsen diffusion; rather, it is micropore diffusion. This is because the diffusion process is combined with mass transfer and exchange between gas (pore void) and MSQ matrix (pore wall). The moisture molecules not only collide with the pore walls but also simultaneously adsorb, desorb, and permeate into the matrix. The average pore size in the film is typically <30 Å; this further explains the small values of diffusivity in the range of 1e-9 cm^2/s, which is much smaller than typical Knudsen diffusivity coefficients.

The results show that the diffusivity coefficient for moisture in MSQ matrix is in the range of 1e-15 cm^2/s. These low diffusivity values confirm that diffusion of moisture through the matrix is primarily through molecular or intralattice cavities and is therefore a highly activated and slow process. The

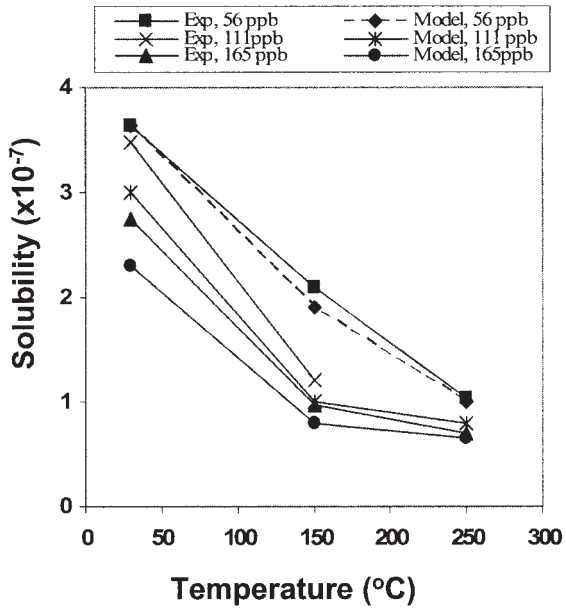

Figure 7. Solubility of moisture in p-MSQ.

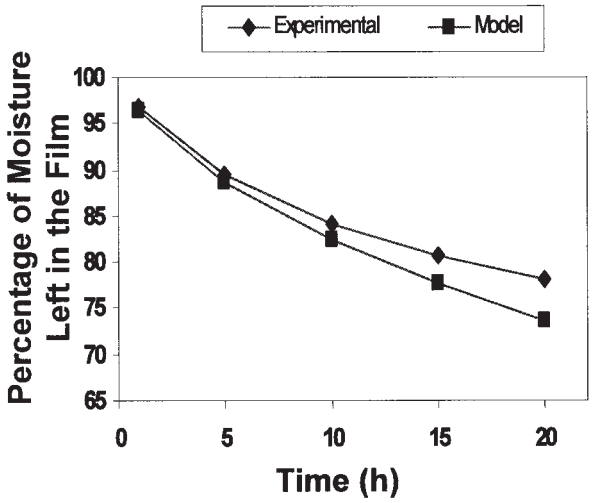

Figure 9. Dependency of moisture residue on purge time.

solubility of moisture in the MSQ matrix (S) was calculated for each case using the sorption loading data. Figure 7 shows that these S values are in good agreement with the values of S determined by fitting the model to desorption data. The result shows a slight dependency of S on moisture concentration. This could be a result of the slight deviation from Henry's law equivalent. The interphase transfer coefficients k_m, k_{ms}, and k_{mg} are weak functions of temperature and are constant for all cases.

Figure 8 gives the moisture content (loading) of the film at different exposure or challenge concentrations. The model results are in good agreement with the experimental data. The results show that at a constant temperature the total moisture loading increases with increasing challenge concentration. In addition, the total amount of moisture sorbed in the film for a particular concentration decreases with increasing temperature. This is because of the decrease in the solubility of moisture in the dielectric film with increase in temperature.

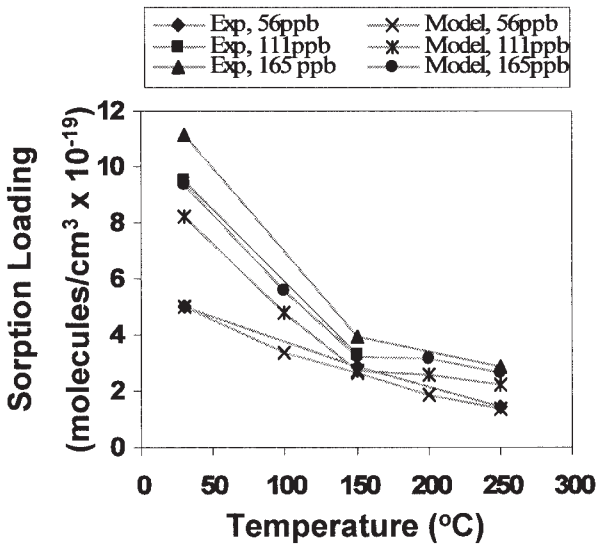

Figure 8. Comparison of model prediction and experimental data on moisture uptake of p-MSQ after exposure to various challenge levels.

Figure 9 compares the percentage of moisture remaining in the film that has been exposed to a challenge moisture concentration of 56 ppb moisture at 150°C; the temporal profile shows the dynamics of the cleanup and desorption as predicted by the model and as measured directly. After 1 h of desorption, only around 5% of the total moisture is removed. Even after 20 h, 75% of the total moisture remains in the dielectric film. This very slow and highly activated overall removal of moisture could be a significant problem in the integration of such porous dielectric films in semiconductor processing, where it is important to have adequate contamination control while maintaining high throughput. The results of this study, and in particular the model, would provide a valuable tool for designing desorption recipes (temperature, gas flow, and gas purity) to ensure effective and efficient cleanup of the dielectric films.

The model is used to study the effect of porosity on the outgassing rate of moisture from the MSQ film. Figure 10 illustrates the outgassing rate for 56 ppb moisture challenge concentration at 30°C over a range of porosity from 20 to 60%. The outgassing rate decreases with increasing porosity; this is because the total amount of moisture sorbed in the film decreases with increasing porosity. However, the decrease in the outgassing rate is not proportional to the increase of porosity, which is explained by various other factors that are also affected by the change in porosity. The overall mass transfer between the film and bulk gas depends on the mass transfer between the pore and bulk gas; an increase in porosity leads to an increase in the mass transport by pores. In fact, two competing factors determine the outgassing rate: film loading and mass transport rate. Figure 10 shows that under conditions used in this study the film loading factor dominates the overall effect.

Figure 11 shows the effect of film thickness on the outgassing dynamics. The thickness affects both the film mass and the

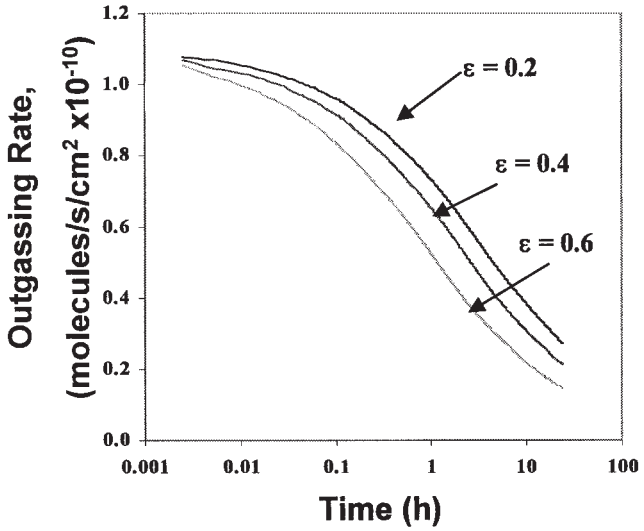

Figure 10. Change in the outgassing rate during moisture desorption.

Sample exposed to and equilibrated with 56 ppb moisture before desorption.

overall diffusional resistance. A decrease in diffusional resistance increases the outgassing rate, whereas a decrease in the total amount of moisture sorbed decreases the outgassing rate. Results show that for very thin films (<0.2 micron in thickness) the effect related to the total amount of moisture is dominant. For films > 0.2 micron the effect of thickness is negligible because most of the early desorption is from a thin top section of the film; only at the late stages of desorption does the effect of film thickness become noticeable.

Conclusion

Sorption, desorption, and transport characteristics of atmospheric gaseous contaminant in general, and moisture in particular, in porous polymeric and dielectric thin films are investigated. In particular, the moisture interactions with p-MSQ are used as model compounds in the study. Moisture incorporation in MSQ matrix involves both hydroxylation reaction and formation of a number of intermediate compounds depending on the exact chemistry of the dielectric matrix. However, for process analysis and engineering applications, the aggregate concentration of intermediates can be represented by an equivalent moisture concentration in the matrix. Moisture sorption and desorption rates in p-MSQ are sensitive to temperature, moisture concentration, film thickness, moisture solubility, and the fundamental properties of moisture transport in the dielectric materials, in the pores and across the solid–gas interphase. The solubility of moisture in MSQ decreases with temperature. The rate of moisture sorption is significantly faster than the rate of moisture desorption under typical processing condition, suggesting a significant potential problem in the removal of moisture and the integration of such low-k dielectric materials in semiconductor processing.

A process model is developed to elucidate the interactions of moisture with porous films. The model is used to analyze the experimental data, determine the fundamental process parameters, and extend the direct measurements to determine the effect of various parameters and process conditions on the moisture removal dynamics. The results show that interphase transport and the pore diffusion coefficients are much smaller than those predicted by bulk or Knudsen diffusion mechanism, thus indicating that the diffusion process is highly activated. The low outgassing rates also indicate that porous films such as p-MSQ are highly susceptible to moisture contamination; the model is a viable tool for developing effective contamination control and cleanup methods and processes.

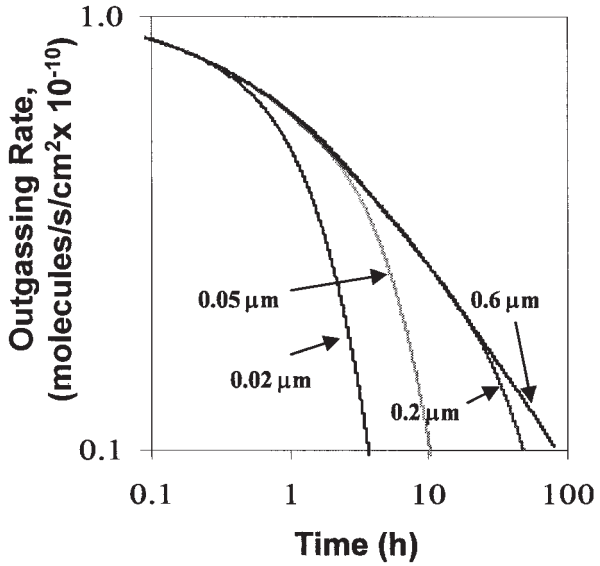

Figure 11. Effect of film thickness on the outgassing rate.

Acknowledgments

The authors are thankful to JSR and International Sematech for providing MSQ material and the coated and treated wafers, and to the NSF/SRC Engineering Research Center for Environmentally Benign Semiconductor Manufacturing for partial support of this research.

Notation

A_{tot} = total exposed surface area available for moisture sorption
C_{film0} = total moisture loading in molecules per unit volume of the film
C_{gb0} = challenge moisture concentration
C_{gb} = concentration of moisture in surrounding medium
$C_{gb,in}$ = concentration of moisture in inlet purge gas stream
C_{gp0} = equilibrium moisture concentration in the pores
C_{gp} = concentration of moisture in pores
C_{s0} = equilibrium moisture concentration in matrix
C_s = concentration of moisture in matrix
D_s = diffusivity of moisture in the matrix
D_g = gas phase diffusivity of moisture in pores
k_m = interphase coefficient between matrix and voids
k_{ms} = interphase transfer coefficient between matrix and gas phase in the surrounding medium
k_{mg} = interphase transfer coefficient between pores and gas phase in the surrounding medium
L = thickness of the film
Q = volumetric flow rate
S = solubility of moisture in the film
S_p = specific surface area of the porous film
V = volume of the reactor
ε = film porosity

Literature Cited

1. Arden W. Future roadblocks and solutions in silicon technology as outlined by ITRS roadmap. *Mater Sci Semicond Process.* 2003;5:313-319.
2. National Institute of Standards and Technology (NIST). Characterization of porous low-k dielectric constant thin films. Gaithersburg, MD: Material Science and Engineering Laboratory, Polymers Division, NIST; Accessed in 2005. http://polymers.msel.nist.gov/projects/project-detail.cfm?PID=11.
3. The International Technology Roadmap for Semiconductors (ITRS). *Update*. San Jose, CA: Semiconductor Association; 2004. May be viewed online at http://public.itrs.net.
4. Tsang CF, Chang CK, Krishnamoorthy A, Ee KY, Su YJ, Li HY, Li WH, Wong LY. A study of post-etch wet clean on electrical and reliability performance of Cu/low k interconnections. *Microelectron Reliability.* 2005;45:517-525.
5. Balakumar S, Wong G, Tsang CF, Hara T, Yoo WJ. Enhancement of adhesion strength of Cu layer on single and multi-layer dielectric film stack in Cu/low k multi-level interconnects. *Microelectron Eng.* 2004;75:183-193.
6. Lu D, Kumar R, Chang CK, Du AY, Wong TKS. Analysis of surface contamination on organosilicate low k dielectric materials. *Microelectron Eng.* 2005;77:63-70.
7. Shamiryan D, Abell T, Iacopi F, Maex K. Low-k dielectric materials. *Mater Today.* 2004;34-39.
8. Louis D, Beverina A, Arvet C, Lajoinie E, Peyne C, Holmes D, Maloney D. Cleaning status on low-*k* dielectric in advanced VLSI interconnect: Characterisation and principal issues. *Microelectron Eng.* 2001;57-58:621-627.
9. Mosig K, Jacobs T, Brennan K, Rasco M, Wolf J, Augur R. Integration challenges of porous ultra low-k spin-on dielectrics. *Microelectron Eng.* 2002;64:11-24.
10. Lloyd JR, Lane MR, Liu XH, Liniger E, Shaw TM, Hu CK, Rosenberg R. Reliability challenges with ultra-low k interlevel dielectrics. *Microelectron Reliability.* 2004;44:1835-1841.
11. Iacopi F, Brongersma SH, Vandevelde B, O'Toole M, Degryse D, Travaly Y, Maex K. Challenges for structural stability of ultra-low-k-based interconnects. *Microelectron Eng.* 2004;75:54-62.
12. Rana N, Raghu P, Shero E, Shadman F. Interactions of moisture and organic contaminants with SiO_2 and ZrO_2 gate dielectric films. *Appl Surf Sci.* 2003;205:160-175.
13. Raghu P, Yim C, Shadman F. Susceptibility of SiO_2, ZrO_2, and HfO_2 dielectrics to moisture contamination. *AIChE J.* 2004;50:1881-1888.
14. Raghu P, Rana N, Yim C, Shero E, Shadman F. Adsorption of moisture and organic contaminants on hafnium oxide, zirconium oxide, and silicon oxide gate dielectrics. *J Electrochem Soc.* 2003;150:186-193.
15. Xie Bo, Muscat AJ. Condensation of silanol groups in porous methylsilsesquioxane films using supercritical CO_2 and alcohol cosolvents. *IEEE Trans Semicond Manuf.* 2004;17:544-553.
16. Bakos T, Rashkeev S, Pantelides S. Reactions and diffusion of water and oxygen molecules in amorphous SiO_2. *Phys Rev Lett.* 2002;88:055508-1: 055508-4.
17. Lomax M. Permeation of gases and vapours through polymer films and thin sheet—Part 1. *Polym Test.* 1980;1:105-147.
18. Crank J, Park GS. *Diffusion in Polymers*. London, UK: Academic Press; 1968.
19. Houst YF. Gas Diffusion through porous media. In: Alexander MG, Arligule G, Ballivy G, Bentur A, Marchand J, eds. *Engineering and Transport Properties of the Interfacial Transition Zone in Cementitious Composites.* Cachan, France: RILEM Publications; 1999:205-217.
20. Vladimir H, Solcova O, Schneider P. Gas permeation in porous solids: Two measurement modes. *Chem Eng Commun.* 2003;190:48-64.
21. Ma C, Haider A, Shadman F. Atmospheric pressure ionization mass spectroscopy for the study of permeation in polymeric tubing. *IEEE Trans Semicond Manuf.* 1993;6:361--366.
22. Anner G. *Planar Processing Primer*. New York, NY: Van Nostrand; 1990.
23. Doremus R. Diffusion of water in silica glass. *J Mater Res.* 1995;10:2379-2389.
24. Verma NK. *Transport and Distribution of Gaseous Impurities in UHP Gas Delivery Systems*. PhD Dissertation. Tucson, AZ: The University of Arizona; 1995.
25. Ni C, San J. Measurement of apparent solid-side mass diffusivity of a water vapor–silica gel system. *Int J Heat Mass Transfer.* 2002;45:1839-1847.
26. Massieon C, Cutler A, Shadman F. Hydrogen reduction of iron-bearing silicates. *Ind Eng Chem Res.* 1993;32:1239-1244.

Manuscript received Sept. 20, 2005, and revision received Nov. 23, 2005.